

# Towards lung EIT image segmentation: Automatic classification of lung tissue state from analysis of EIT monitored recruitment manoeuvres

Bartłomiej Grychtol<sup>1</sup>, Gerhard K Wolf<sup>2</sup>, Andy Adler<sup>3</sup> and John H Arnold<sup>2</sup>

<sup>1</sup> Department of Bioengineering, University of Strathclyde, Rottenrow, Glasgow G4 0NW, UK

<sup>2</sup> Division of Critical Care Medicine, Department of Anesthesia, Children's Hospital Boston, Harvard Medical School, Boston, MA 02115, USA

<sup>3</sup> Systems and Computer Engineering, Carleton University, Ottawa, ON K1S 5B6, Canada

E-mail: bartlomiej.grychtol@strath.ac.uk

**Abstract.** There is emerging evidence that the ventilation strategy used in acute lung injury (ALI) makes a significant difference in outcome and that an inappropriate ventilation strategy may produce ventilator-associated lung injury. Most harmful during mechanical ventilation are lung overdistension and lung collapse or atelectasis. Electrical Impedance Tomography (EIT) as a non-invasive imaging technology may be helpful to identify lung areas at risk. Currently no automated method is routinely available to identify lung areas that are overdistended, collapsed or ventilated appropriately. We propose a fuzzy logic based algorithm to analyse EIT images obtained during stepwise changes of mean airway pressures during mechanical ventilation. The algorithm is tested on data from two published studies of stepwise inflation-deflation manoeuvres in an animal model of ALI using conventional and high frequency oscillatory ventilation. The timing of lung opening and collapsing on segmented images obtained using the algorithm during an inflation-deflation manoeuvre are in agreement with well known effects of surfactant administration and changes in shunt fraction. While the performance of the algorithm has not been verified against a gold standard, we feel that it presents an important first step in tackling this challenging and important problem.

*Keywords:* EIT, overdistention, collapse, mechanical ventilation, monitoring, fuzzy logic  
Submitted to: *Physiol. Meas.*

## 1. Introduction

We present an automated method to analyse Electrical Impedance Tomography (EIT) images obtained during stepwise changes of mean airway pressures during mechanical

ventilation. This method may be useful in determining changes in lung conditions, such as atelectasis or overdistension.

There is emerging evidence that the ventilation strategy used in acute lung injury (ALI) makes a significant difference in outcome and that an inappropriate ventilation strategy may produce ventilator-associated lung injury. In a retrospective study, 24% of patients who did not have ALI at the onset of ventilation developed ALI after a mean of 2.5 days of mechanical ventilation (Gajic et al. 2004). Most harmful during mechanical ventilation are lung overdistension (causing disruption of alveoli) and lung collapse or atelectasis (leading to hypoxia and atelectrauma by repeated opening and closing of lung units). Both overdistension caused by excessively high airway pressures (Imai & Slutsky 2005) as well as cyclic recruitment and derecruitment (Chu et al. 2004) caused by insufficient end expiratory pressures add to the development of ventilator induced lung injury. Current lung protective strategies of ventilation are targeted towards reducing overdistension and achieving adequate lung opening.

As ALI is a heterogeneous disease, and regional differences in lung compliance are associated with distinct regional differences in lung opening and closing (Gattinoni et al. 2006), EIT as a non-invasive imaging technology may be helpful to identify lung areas at risk. No other method can provide non-invasive assessment of regional lung volumes in real time at the bedside. Other methods to assess lung volumes such as respiratory inductive plethysmography provide only global, not regional, assessment of lung volume. Advanced imaging techniques such as positron emission tomography and computed tomography are not feasible to be used as a continuous bedside monitor. However, no automated method is routinely available to identify from EIT tomograms lung areas that are overdistended, collapsed or ventilated appropriately.

Regional changes in air content of the lungs (ventilation) produce large changes in the conductivity distribution which can be imaged with EIT. Several studies have shown that EIT is able to map regional differences in lung behaviour. For example, Frerichs et al. (2003) showed in an animal model of acute lung injury during conventional ventilation that the dependent lung regions respond more slowly to recruitment manoeuvres, and this effect was ameliorated with exogenous surfactant. In an animal model of acute lung injury during HFOV, non-dependent lung areas showed significantly decreased regional ventilation-induced impedance changes at higher mean airway pressures (MAP), suggesting overdistension, whereas dependent lung areas showed increased impedance changes, suggesting recruitment (Wolf et al. 2010).

While EIT shows exciting potential as a tool to measure the regional information necessary to help optimize lung ventilation, little work has been done to develop a strategy to summarize and present the most relevant clinical information. Consider the common scenario where the physician chooses to change the PEEP (positive end-expiratory pressure) level for a patient. A modern ventilator will show immediately the change in global lung compliance, and within several minutes, the effect of the change can be seen on arterial blood gasses. However, the questions that one would like to answer are: have new lung regions opened? are some regions now overdistended? have

any parts of the lung collapsed? Using the term “lung state” to refer to lung which is normal, collapsed, etc., we are looking for a technique to identify lung states and in particular the changes in state.

In this paper, we propose a method to generate images of the changes in lung states from EIT images during stepwise changes in mean airway pressure. We propose a fuzzy logic based algorithm to classify the images, and show its performance for images from conventional and high frequency oscillatory ventilation. In the context of EIT, fuzzy logic has previously been used to distinguish the lungs and the heart in EIT images during ventilation and apnea in an animal model (Tanaka et al. 2008).

The objective of this study is to propose a theoretically-derived lung tissue state classification algorithm to be used with the current mainstream EIT technology. As such, validation against a gold-standard technique such as CT is outside the scope of this study. In the rest of the paper, we describe our method, show its performance, and discuss the applications in which it performs well and the remaining challenges with such classification approaches.

## 2. Methods

### 2.1. EIT data and algorithms

The algorithm designed in this study is tested on data from previous published studies by Frerichs et al. (2003), a conventional ventilation study, and Wolf et al. (2010), a similar study with high-frequency oscillatory ventilation (HFOV). Both studies used the Göttingen Goe-MF II system during a stepwise recruitment-derecruitment manoeuvre in a porcine model of lung injury. Sixteen electrodes were applied circumferentially around the animal’s chest. Table 1 summarises the design of these studies.

For the purpose of this paper, the raw data from both studies were reconstructed into EIT images with the GREIT algorithm using the cylindrical model (Adler et al. 2009). Prior to reconstruction, surface electrode readings were normalised to a reference recording. Thus, the reconstructed conductivity images are unitless. For the study by Frerichs et al. (2003) the reference was a short period at the end of a 30 second apnea (disconnection from the ventilator) before the onset of the manoeuvre and after the induction of lung injury. This is in contrast with the data from our study (Wolf et al. 2010), where a recording of ventilation prior to the induction of injury was used as reference.

Short recordings of ventilation at each pressure step of the recruitment-derecruitment manoeuvre in both studies were selected for analysis. Functional EIT (fEIT) images were calculated for each step. For conventional ventilation, fEIT images were obtained by calculating the amplitude of the strongest ventilation-related frequency component of the time-course signal in each pixel. For HFOV, due to the small amplitude of ventilation-induced changes relative to those caused by the heartbeat, rather than using the amplitude of the relevant peak on the spectrum, the average power

Table 1: Summary of data sources.

Study	Animal	Intervention	Reference	EIT
Frerichs et al. (2003)	Newborn piglet (body weight: 2kg); lung injury induced with lavage	Conventional ventilation at 10 ml/kg with PEEP between 0 and 30 cm H <sub>2</sub> O increased and then decreased in steps of 5 cm H <sub>2</sub> O over 120 seconds. Measurements recorded after induction of lung injury and following surfactant administration.	End of a 30 seconds period of apnea.	Goe-MF II, acquisition rate: 13 Hz, 16 electrodes
Wolf et al. (2010)	Yorkshire swine (body weight: 15kg); lung injury induced with lavage	HFOV ventilation at 10 Hz with MAP between 15 and 40 cm H <sub>2</sub> O increased and then decreased in steps of 5 cm H <sub>2</sub> O in 15 minutes intervals.	Conventional ventilation prior to lung injury	Goe-MF II, acquisition rate: 44 Hz, 16 electrodes

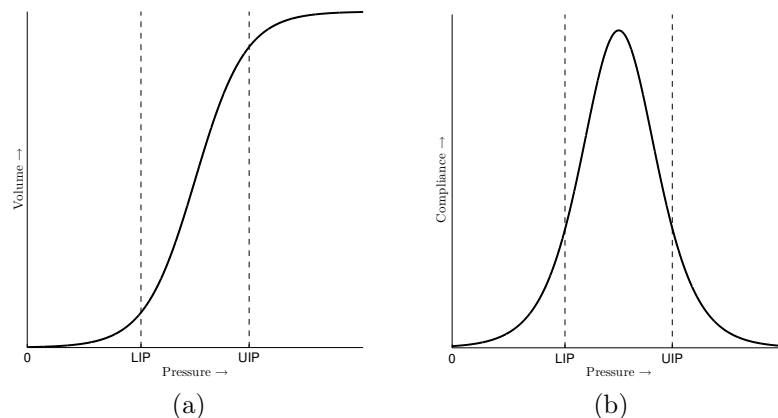


Figure 1: (a) Idealized pressure-volume curve using the equation of Venegas et al. (1998) and (b) the corresponding compliance (as first derivative of volume) vs. pressure relationship. Inflection points were calculated using the method described in Grychtol et al. (2009).

within a 1 Hz band around the peak was calculated to construct the fEIT image. This method avoids some of the problems caused by spectral leakage and is fully described in Wolf et al. (2010).

## 2.2. Lung tissue states

We previously demonstrated that lung volumes corresponding to individual pixels of EIT images exhibit the same basic pressure-volume characteristic as the lung as a whole (a sigmoidal pressure-volume/impedance curve) (Grychtol et al. 2009). The inflection points divide the pressure-volume curve into three distinct areas (c.f. figure 1). At low pressures, and below the lower inflection point (LIP), the lung is predominantly collapsed and is characterized by low volume and compliance. Conversely, above the upper inflection point (at high pressures), the lung is predominantly in the overdistended state characterized by high volume and low compliance. Between the LIP and the UIP lung is in its normal, open state with medium volume and moderate to high compliance. In this study, we apply these definitions to lung volumes corresponding to individual pixels of EIT images.

## 2.3. Effect of a change in pressure

The main challenge in classifying lung tissue states from EIT data is to distinguish between collapsed and overdistended areas without performing a pressure-volume manoeuvre. Recent reports show that functional EIT (fEIT) imaging can provide reliable information regarding the distribution of ventilation (e.g. Frerichs et al. 2002, Hinz et al. 2003, Victorino et al. 2004). Areas of low compliance exhibit little ventilation-induced change, and are thus easy to identify on fEIT images. However, absolute impedance, and hence air volume, information would be required to distinguish areas that are overdistended from those that are collapsed. In normalised difference EIT, absolute impedance information is not available, and the unitless value of “relative  $\Delta Z$ ” is generally not informative. A different feature is therefore required to distinguish collapsed and overdistended areas.

Because fEIT images reflect local compliance, comparing ventilation recordings before and after an adjustment in the baseline pressure during mechanical ventilation (peak end-expiratory pressure, PEEP, for conventional ventilation, or mean airway pressure, MAP, for HFOV) should reveal the sign of the pressure-compliance relationship. This, in turn, will allow distinguishing the two “inactive” states. As depicted on figure 1(b), below the LIP, an increase in pressure leads to increased compliance as more units within a given region of lung open up. Above the UIP, the relationship is reversed — an increase in pressure leads to decrease in compliance. Conversely, when the pressure is decreased, compliance increases in overdistended areas and diminishes in collapsed ones.

While additional features (discussed below) are required for adequate performance, this idea is central to the algorithm presented here. The data from stepwise recruitment-derecruitment manoeuvres conducted by Frerichs et al. (2003) and Wolf et al. (2010) provide ample opportunity to test the performance of this algorithm.

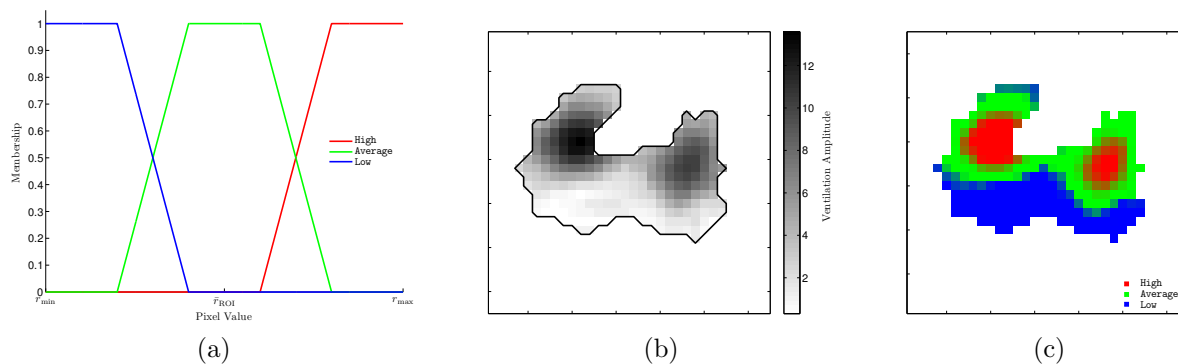


Figure 2: (a) Fuzzy membership functions for the three fuzzy sets. The membership of a pixel  $r$  depends on its value with respect to the mean,  $\bar{r}_{ROI}$ , and the extreme values,  $r_{\min}$  and  $r_{\max}$ , within the ROI; (b) A typical fEIT image (data from Frerichs et al. (2003)), conventional ventilation PEEP 15 cm H<sub>2</sub>O); and (c) the corresponding image of fuzzy set membership.

#### 2.4. Constructing features

The ventilation-induced impedance changes that constitute fEIT images are unitless and ultimately depend on the choice of reference recording used for reconstruction. As such, it is impossible to define meaningful thresholds for normal values. Hence, the ventilation-induced impedance change in a volume of lung corresponding to an individual EIT pixel can only be assessed by comparison with the values in the rest of the lung.

This necessitates the ability to distinguish lung from other tissues in EIT images. Several approaches to defining such regions of interest (ROI) have been used to date (see Pulletz et al. 2006). In this study, we employ the technique based on comparing linear regression coefficients of individual pixel's impedance signal against the average signal of the entire image. To achieve maximum fidelity, for the analysis of the data from the study of Wolf et al. (2010) a recording of a pressure-volume manoeuvre before induction of lung injury was used for ROI definition, as described therein. For the study of Frerichs et al. (2003), only data recorded after lung injury is available and thus an entire recording was used to derive the ROI. As recommended by Pulletz et al. (2006), a threshold value of 20% of the maximum regression coefficient found was used to delineate the lung ROI.

To facilitate assessment, fEIT images are normalized with respect to the mean of the lung ROI. After normalization, values in individual pixels are assigned a degree of membership,  $\mu(x)$ , to the fuzzy sets **Low**, **Hi**, and **Average** (abbreviated **Lo**, **Hi** and **Avg** respectively) through the process of fuzzification according to figure 2(a). We chose to use fuzzy sets rather than predicate inference rules in the algorithm presented here due to the ability of the former to formalize linguistic reasoning in a form that is both easy to understand and suitable for use in situations where crisp thresholds are difficult to define. Fuzzy sets can easily be extended or incorporated into fuzzy logic control systems

(see Mendel 1995 for a comprehensive tutorial), such as that reported by Luepschen et al. (2007). We adopted the following definitions for fuzzy set intersection, union and complement:

$$\mu_{A \cap B}(x) = \min(\mu_A(x), \mu_B(x)) \quad (1)$$

$$\mu_{A \cup B}(x) = \max(\mu_A(x), \mu_B(x)) \quad (2)$$

$$\mu_{A^c}(x) = 1 - \mu_A(x) \quad (3)$$

where  $\mu_A$  is the membership function for the fuzzy set  $A$ ,  $A^c$  denotes the complement of  $A$ , and  $x$  belongs to the domain of the function. It follows from the membership functions defined in figure 2(a) that

$$\mu_{Lo}(x) + \mu_{Avg}(x) + \mu_{Hi}(x) = 1 \quad (4)$$

for all  $x$  in  $[-1, 1]$ . With  $A$ ,  $B$  and  $C$  representing any combination of **Low**, **Average** and **High**, it also holds that

$$\mu_{C^c}(x) = 1 - \mu_C(x) = \mu_A(x) + \mu_B(x), \quad (5)$$

which, in this case, is a more intuitive equivalent of the linguistic “A or B” than the fuzzy union defined above. Thus, the algorithm presented here is defined in terms of intersection and complement only.

Figure 2(c) shows a typical fEIT image (figure 2(b)) after fuzzification. Each pixel in the image is colored according to the values of its membership in the three sets, such that pixels belonging to the set **Average** are green, and those belonging to the sets **Hi** and **Low** are coded as red and blue, respectively. Note the smooth transition between the differently coloured areas.

After normalization and fuzzification, the fEIT images are ready for use as features in a classification algorithm. In the same fashion, we have extracted features from the difference between fEIT images at consecutive pressure steps ( $\Delta$ fEIT images). Images of mean conductivity (for HFOV) and PEEP conductivity (for conventional ventilation) over the same time periods as the fEIT images were also computed and processed analogously. Additionally, a fuzzy version of the sign function (sgn) has been developed, such that the sign (direction) of change in either ventilation-induced conductivity change or mean conductivity can be used as a feature. For simplicity the same fuzzy set abbreviations will be used for the sign function with the understanding that **High** values are positive, **Low** — negative, and **Average** — close to zero. Thus, for each step change in pressure, eight features are derived from EIT data, as summarised in table 2. One additional feature is the direction of change in pressure (increase or decrease).

For the sake of simplifying notation, from this point on we will treat **Lo**, **Hi** and **Avg** (and their complements) as unary operators acting on features, such that  $Hi[fEIT(n)]$  and  $Lo^c[fEIT(n)]$  will denote the fuzzy set of pixels in ROI whose value of ventilation-induced conductivity change at the  $n$ -th pressure step is **High** and not **Low**, respectively.

Table 2: Summary of features used for classification.

Feature	Description
fEIT( $n$ )	Functional image at $n$ -th pressure step. Computed based on spectral analysis of a short recording of ventilation (see subsection 2.1 for details).
fEIT( $n - 1$ )	Functional image one step before $n$ .
$\Delta$ fEIT( $n$ )	fEIT( $n$ ) – fEIT( $n - 1$ ). Change in ventilation induced conductivity change caused by a change in pressure
sgn( $\Delta$ fEIT( $n$ ))	Sign of change in magnitude of ventilation induced conductivity changes
$\sigma(n)$	Baseline conductivity (mean for HFOV and PEEP level for conventional ventilation) at $n$ -th pressure step.
$\sigma(n - 1)$	Baseline conductivity one step before $n$ .
$\Delta\sigma(n)$	$\sigma(n) - \sigma(n - 1)$ . Change in conductivity induced by a step change in pressure.
sgn( $\Delta\sigma(n)$ )	Sign of change in conductivity.
sgn( $\Delta p$ )	$p(n) - p(n - 1)$ Sign of change in pressure, $p$ , between steps $n - 1$ and $n$ .

### 2.5. Event detection

Using the features described above, we defined four events of interest that reveal the state of the volume of lung corresponding to a particular EIT pixel. For a positive change in pressure, these are the *opening* of collapsed areas and *overdistending* of previously perfectly functional areas. Conversely, when pressure is decreased, previously ventilated areas could be *collapsing*, while overdistended regions could be *recovering*. In general, the events concern either an inactive pixel becoming active, or an active pixel becoming inactive (i.e. not ventilated). We define not ventilated pixels as those whose value of ventilation induced conductivity change belongs to the Low fuzzy set, and all others as active. When an inactive pixel becomes active (more ventilated) as a result of a positive change in pressure and its conductivity decreases, it is recognised as a previously not ventilated area of the lung that is *opening*. Hence, the fuzzy set **Opening** is defined as:

$$\begin{aligned} \mathbf{Opening}(n) = & \text{Lo}[\text{fEIT}(n - 1)] \cap \text{Lo}^{\text{c}}[\text{fEIT}(n)] \cap \text{Hi}[\text{sgn}(\Delta\text{fEIT}(n))] \\ & \cap \text{Lo}[\text{sgn}(\Delta\sigma(n))] \cap \text{Hi}[\text{sgn}(\Delta p)] . \end{aligned} \quad (6)$$

The other three events are defined in a similar fashion as an intersection of several features and are summarised in table 3.

### 2.6. Event resolution and image segmentation

Because the definitions of events are not mutually exclusive, at times more than one event is detected (i.e. has a nonzero fuzzy membership value) in a given pixel. In these instances, the event with the highest membership value is preserved, and the rest are ignored. This is the simplest form of defuzzification.

Table 3: Event definitions. Each event is a fuzzy intersection of the feature sets listed.

Feature	Opening	Collapsing	Overdistending	Recovering
fEIT( $n$ )	Lo <sup>C</sup>	Hi <sup>C</sup>	Hi <sup>C</sup>	Lo <sup>C</sup>
fEIT( $n - 1$ )	Lo	Lo	Lo <sup>C</sup>	Hi <sup>C</sup>
$\Delta$ fEIT( $n$ )			Lo	
sgn( $\Delta$ fEIT( $n$ ))	Hi	Lo	Lo	Hi
sgn( $\Delta\sigma(n)$ )	Lo	Hi	Lo	Hi
sgn( $\Delta p$ )	Hi	Lo	Hi	Lo

Once all events associated with a given pressure step are recognised, two images are produced — one for each pressure value — such that pixels recognised as representing overdistended areas are red, collapsed areas — blue, those in normal state are green, and those that are inactive, but cannot be classified, are magenta. The “severity” of each recognised pathological state is determined by the degree of membership in the Lo[fEIT] fuzzy set and is reflected by the intensity of the corresponding color. Thus, in essence, the resultant images are segmented functional EIT images.

### 3. Results

The classification algorithm described above has been applied to data sets from stepwise inflation-deflation manoeuvres performed in a porcine model of lung injury during conventional (Frerichs et al. 2003) and high frequency oscillatory ventilation (Wolf et al. 2010). We present classifications obtained from each pressure step in isolation, as well as comprehensive reconstructions of the state of the lung throughout the manoeuvres integrating classification results from all pressure changes.

#### 3.1. Conventional ventilation

The study of Frerichs et al. (2003) compared the changes in distribution of ventilation during an inflation-deflation manoeuvre before and after surfactant treatment. The events detected during both manoeuvres are presented in figure 3. After surfactant treatment, the majority of the lung opens between PEEP of 5 and 15 cm H<sub>2</sub>O while before surfactant administration, the bulk of the lung opens up only at PEEP of 20 cm H<sub>2</sub>O.

For the first manoeuvre, the classification made possible by information from each pressure change individually is presented in figure 4. In most cases, areas that remain not ventilated after the change cannot be classified correctly. In particular, at lower pressures during the inflation limb, lung areas which later open up and hence must be collapsed are initially classified as overdistended. During the deflation limb, areas that have been previously identified as collapsed (during the change in PEEP from 15 to 10 cm H<sub>2</sub>O) are later difficult to assign to a specific lung state and are marked as ventilated.

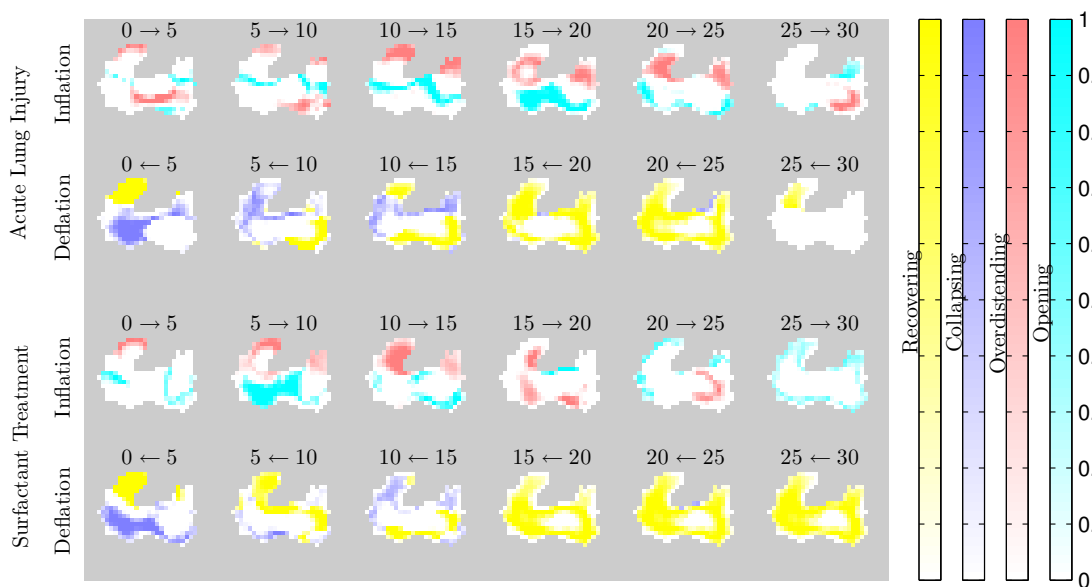


Figure 3: Events detected during a stepwise PEEP recruitment and derecruitment manoeuvre in a piglet with ALI before (top) and after (bottom) surfactant treatment, as described in Frerichs et al. (2003). Arrows indicate direction of transition between two levels of PEEP expressed in  $\text{cm H}_2\text{O}$ .

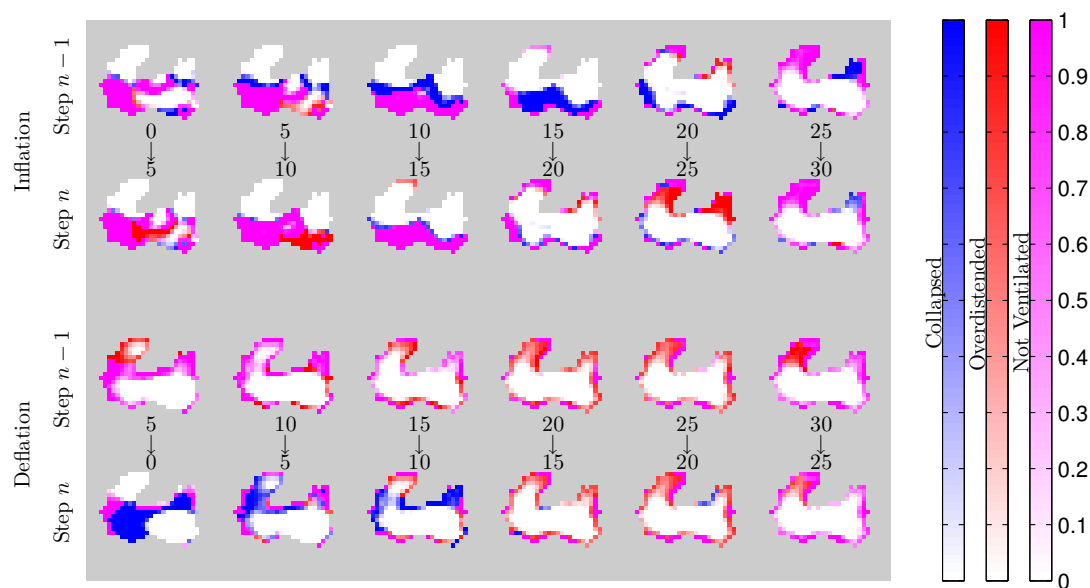


Figure 4: Lung state classification in a piglet with ALI based on the events presented in figure 3. Classification was performed separately for each pressure change using only information from EIT recordings before and after the change.

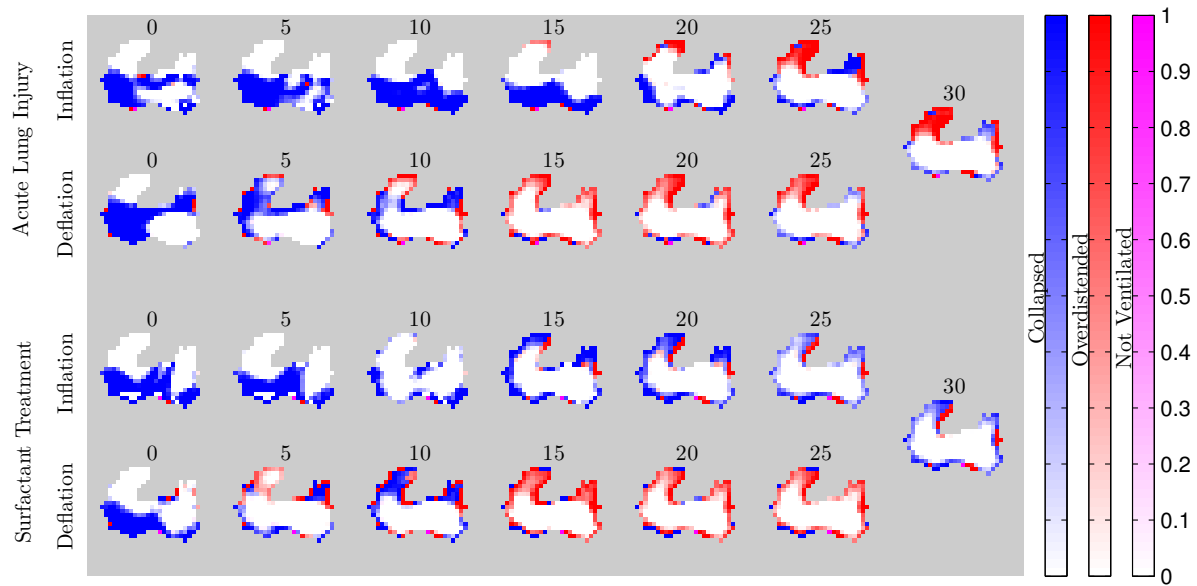


Figure 5: Reconstruction of the state of the lung integrating classification results from all PEEP changes (c.f. figure 3).

This indicates the need to keep previous classification results in memory and integrate them with information from the current step change in pressure. In figure 5, results of integrating information from all pressure steps are presented. In an attempt to reconstruct the state of the lung at each pressure, in addition to remembering states recognised earlier, classification at previous pressure steps is retrospectively updated. Thus, areas of lung that only open during a change of PEEP from 15 to 20 cm H<sub>2</sub>O are marked as collapsed for all PEEP values up to 20 cm H<sub>2</sub>O despite the algorithm not being able to classify them at earlier steps.

The reconstructed results show that before surfactant treatment the lung requires higher PEEP levels to recruit and maintain in that state. In comparison, after surfactant treatment, the lung opens up (during the inflation limb) and collapses (during deflation) at lower PEEP levels. Additionally, at each PEEP level, a smaller fraction of lung is in the collapsed state. This is consistent with the observations of Frerichs et al. (2003) and reflects well known physiological effects of surfactant administration in ALI (Whitsett & Weaver 2002).

### 3.2. High frequency oscillatory ventilation

Figure 6 presents the events detected during a stepwise inflation-deflation manoeuvre in a porcine model of ALI during HFOV (Wolf et al. 2010). During inflation, at lower values of MAP, lung opening in dependent areas of the lung is accompanied by overdistention in the nondependent part of the left lung. However, this only becomes visible in the reconstructed state of the lung throughout the manoeuvre (figure 7) at higher MAP values (MAP 25–30 cm H<sub>2</sub>O) due to the initially high values of ventilation-induced

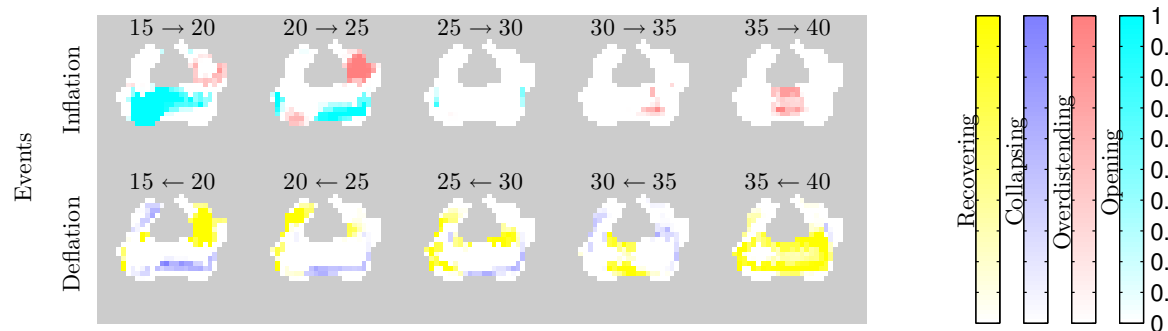


Figure 6: Events detected during a MAP inflation-deflation manoeuvre during HFOV (Wolf et al. 2010). Arrows indicate direction of transition between two levels of MAP expressed in  $\text{cm H}_2\text{O}$ .

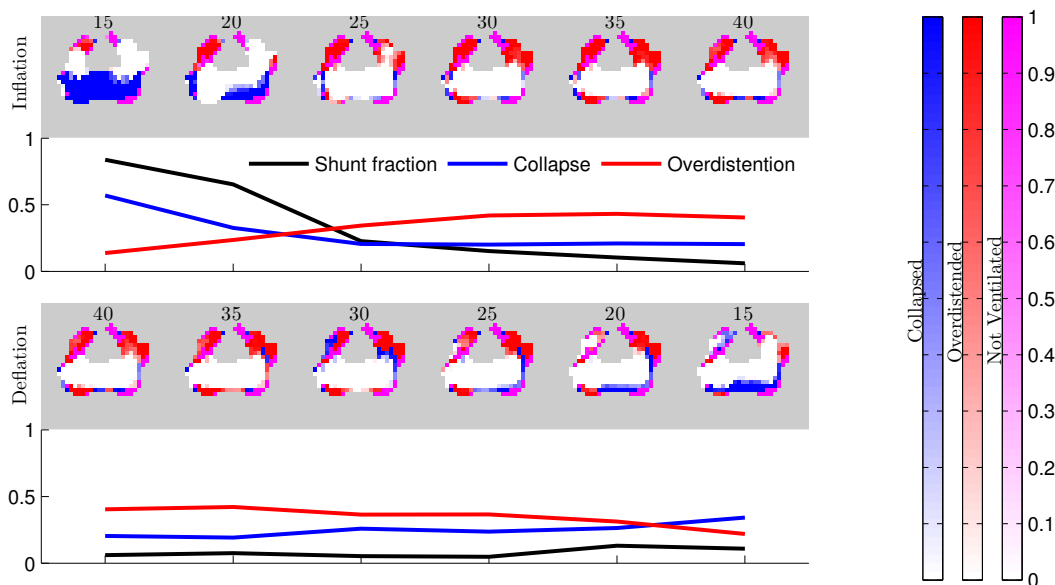


Figure 7: *Images*: Reconstruction of the state of the lung integrating classification results from all MAP changes (c.f. figure 6). *Graphs*: Fraction of lung classified as collapsed and overdistended compared with the shunt fraction.

changes in this area.

The amount of collapsed and overdistended lung (calculated as average membership value for the respective classes within the ROI) is compared against the shunt fraction in the plots in figure 7. According to the classification results, a significant part of the lung is collapsed at MAP 15  $\text{cm H}_2\text{O}$  and most of it is recruited at MAP 25  $\text{cm H}_2\text{O}$ . This is confirmed by the shunt fraction which falls from 0.83 to 0.23 between MAP 15 and 25  $\text{cm H}_2\text{O}$ . During the deflation part most of the lung remains recruited and only a small fraction is classified as collapsed at MAP 15. Corroborating this, the shunt fraction rises only slightly from 0.06 at MAP 40 to 0.10 at MAP 15.

## 4. Discussion

We present an algorithm that attempts to identify collapsed and overdistended lung tissue by analyzing changes in EIT recordings induced by adjusting pressure settings during mechanical ventilation. This is the first attempt at segmentation of the fEIT images of the lungs. The results of applying the algorithm to data sets from inflation-deflation manoeuvres match expectations in terms of amount and timing of lung collapse and opening. The fact that the algorithm performs reasonably well for both conventional and high frequency oscillatory ventilation, demonstrates that the chosen features are not specific to the type of ventilation. While we recognize that the performance of the algorithm has not been verified and requires further work, we feel that it presents an important first step in tackling this challenging and important problem.

The algorithm assumes that overdistention and opening can only occur during a positive change in pressure, while lung collapse or recovery from overdistention only occur during a negative change. This causes the algorithm to misinterpret changes in ventilation distribution that result from re-balancing of pressures and volumes within the lung (“Pendelluft”), e.g. the non-dependent area of the left lung during the change from PEEP 25 to 30 before surfactant administration (figure 3). This assumption should be relaxed in order to capture the full dynamics of re-distribution of air content and tidal volume as a result of change in pressure. This, in turn, will necessitate a more sophisticated defuzzification procedure than employed here (see 2.6).

Changes in poorly ventilated areas appear to be particularly challenging to classify correctly. An example of that can be seen on figure 4 at lower values of PEEP during inflation, where dependent part of the left lung is incorrectly identified as overdistended. The **overdistending** event was detected because the area exhibited a small increase in conductivity while its ventilation-induced conductivity changes decreased. This problem could be resolved if static air volume information was available on top of the functional EIT images. As mentioned before, in normalized difference imaging, conductivity values are in general not informative due to their strong dependence on the reference recording. However, if the entire lung could be assumed to be in the same state during the reference recording, the conductivity values could become informative. The reference recordings used in this study do not satisfy this condition. During apnea, parts of the lung collapse completely while others remain open. Similarly, in healthy lung not all units are recruited at atmospheric pressure. We speculate that using a reference recording obtained during a short period of maximal recruitment could be helpful in distinguishing collapsed and overdistended areas even when they remain not ventilated.

Cardiopulmonary interactions may influence lung EIT measurements. High mean airway pressures can compromise pulmonary blood flow, and may decrease venous return to the right side of the heart. We reduced the influence of heart filling on the EIT data by excluding the heart region from the ROI. Increase in air volume and reduction of pulmonary blood flow both lead to decreased lung conductivity (increased lung impedance). Superposition of these effects can lead to a larger decrease in

local conductivity than could be explained by change in air volume alone, potentially decreasing the sensitivity of a classification algorithm to lung overdistention. We try to avoid this pitfall by not using the magnitude of conductivity change as a feature in the algorithm described here. Instead, we use features derived from functional EIT images and only the sign of the conductivity change —  $\text{sgn}(\Delta\sigma(n))$ .

Using a single change in pressure, the algorithm can only provide information about the areas of the lung where events were detected (figure 3). As demonstrated by the reconstructions in figures 5 and 7, retaining information from previous classifications and incorporating it into the algorithm could help produce more complete images at each pressure step.

The process of fuzzification used in the current algorithm compares the value of each pixel to the mean and range of the values within the ROI for that image. At times, this leads to counter-intuitive results, such as the “collapsing” event detected in the non-dependent part of the right lung during decrease of PEEP from 15 to 10 cm H<sub>2</sub>O in an animal with ALI (figure 3). It would be better if magnitude of ventilation-induced changes in each pixel could be assessed with respect to the range of previously observed values in that pixel, especially if EIT was used for long term monitoring of mechanical ventilation.

#### 4.1. Limitations

The classification algorithm requires a priori knowledge of which pixels on the EIT image correspond to the lungs. In the animal study using HFOV, the ROI was obtained from data during a PV manoeuvre before lung injury. In the clinical context, and for the conventional ventilation study, there is no guarantee that all regions of the lung recruit during such manoeuvres, and hence the resulting ROI may be incomplete.

We used no secondary confirmation technique to verify the observed findings, but in previous studies relative impedance changes have been highly correlated with changes in air content seen on CT in animals (Frerichs et al. 2002) and humans (Victorino et al. 2004).

## Acknowledgements

The authors would like to thank Inéz Frerichs and coworkers for sharing their data. The data is available on the EIDORS website (<http://eidors3d.sourceforge.net>) under the Creative Commons Artistic License (with Attribution).

## References

- Adler A, Arnold J H, Bayford R, Borsic A, Brown B, Dixon P, Faes T J, Frerichs I, Gagnon H, Gärber Y, Grychtol B, Hahn G, Lionheart W R B, Malik A, Patterson R P, Stocks J, Tizzard A, Weiler N & Wolf G K 2009 *Physiol Meas* **30**(6), S35—S55.

- Chu E K, Whitehead T & Slutsky A S 2004 *Crit Care Med* **32**(1), 168–74. 0090-3493 Journal Article.  
[http://www.ncbi.nlm.nih.gov/entrez/query.fcgi?cmd=Retrieve&db=PubMed&dopt=Citation&list\\_uids=14707576](http://www.ncbi.nlm.nih.gov/entrez/query.fcgi?cmd=Retrieve&db=PubMed&dopt=Citation&list_uids=14707576)
- Frerichs I, Dargaville P A, Dudykevych T & Rimensberger P C 2003 *Intensive Care Med* **29**(12), 2312–6.  
[http://www.ncbi.nlm.nih.gov/entrez/query.fcgi?cmd=Retrieve&db=PubMed&dopt=Citation&list\\_uids=14566457](http://www.ncbi.nlm.nih.gov/entrez/query.fcgi?cmd=Retrieve&db=PubMed&dopt=Citation&list_uids=14566457)
- Frerichs I, Hinz J, Herrmann P, Weisser G, Hahn G, Dudykevych T, Quintel M & Hellige G 2002 *J Appl Physiol* **93**(2), 660–6. 8750-7587 Journal Article.  
[http://www.ncbi.nlm.nih.gov/entrez/query.fcgi?cmd=Retrieve&db=PubMed&dopt=Citation&list\\_uids=12133877](http://www.ncbi.nlm.nih.gov/entrez/query.fcgi?cmd=Retrieve&db=PubMed&dopt=Citation&list_uids=12133877)
- Gajic O, Dara S I, Mendez J L, Adesanya A O, Festic E, Caples S M, Rana R, St Sauver J L, Lymp J F, Afessa B & Hubmayr R D 2004 *Crit Care Med* **32**(9), 1817–24. 0090-3493 Journal Article Multicenter Study.  
[http://www.ncbi.nlm.nih.gov/entrez/query.fcgi?cmd=Retrieve&db=PubMed&dopt=Citation&list\\_uids=15343007](http://www.ncbi.nlm.nih.gov/entrez/query.fcgi?cmd=Retrieve&db=PubMed&dopt=Citation&list_uids=15343007)
- Gattinoni L, Caironi P, Cressoni M, Chiumello D, Ranieri V M, Quintel M, Russo S, Patroniti N, Cornejo R & Bugeo G 2006 *N Engl J Med* **354**(17), 1775–86.  
[http://www.ncbi.nlm.nih.gov/entrez/query.fcgi?cmd=Retrieve&db=PubMed&dopt=Citation&list\\_uids=16641394](http://www.ncbi.nlm.nih.gov/entrez/query.fcgi?cmd=Retrieve&db=PubMed&dopt=Citation&list_uids=16641394)
- Grychtol B, Wolf G K & Arnold J H 2009 *Physiol Meas* **30**(6), S137–S148.
- Hinz J, Neumann P, Dudykevych T, Andersson L G, Wrigge H, Burchardi H & Hedenstierna G 2003 *Chest* **124**(1), 314–322.  
<http://www.chestjournal.org/cgi/content/abstract/124/1/314>
- Imai Y & Slutsky A S 2005 *Critical Care Medicine* **33**(3), S129–34.
- Luepschen H, Meier T, Grossherr M, Leibecke T, Karsten J & Leonhardt S 2007 *Physiological Measurement* **28**(7), S247–S260.  
<http://stacks.iop.org/0967-3334/28/S247>
- Mendel J 1995 *Proceedings of the IEEE* **83**(3), 345–377.
- Pulletz S, van Genderingen H R, Schmitz G, Zick G, Schadler D, Scholz J, Weiler N & Frerichs I 2006 *Physiol Meas* **27**(5), S115–27. 0967-3334 (Print) Journal Article.  
[http://www.ncbi.nlm.nih.gov/entrez/query.fcgi?cmd=Retrieve&db=PubMed&dopt=Citation&list\\_uids=16636403](http://www.ncbi.nlm.nih.gov/entrez/query.fcgi?cmd=Retrieve&db=PubMed&dopt=Citation&list_uids=16636403)
- Tanaka H, Ortega N, Galizia M, Borges J & Amato M 2008 *Clinics (Sao Paulo)* **63**(3), 363–70.
- Venegas J G, Harris R S & Simon B A 1998 *J Appl Physiol* **84**(1), 389–395.  
<http://jap.physiology.org/cgi/content/abstract/84/1/389>
- Victorino J A, Borges J B, Okamoto V N, Matos G F, Tucci M R, Carames M P, Tanaka H, Sipmann F S, Santos D C, Barbas C S, Carvalho C R & Amato M B 2004 *Am J Respir Crit Care Med* **169**(7), 791–800. 1073-449x Journal Article.  
[http://www.ncbi.nlm.nih.gov/entrez/query.fcgi?cmd=Retrieve&db=PubMed&dopt=Citation&list\\_uids=14693669](http://www.ncbi.nlm.nih.gov/entrez/query.fcgi?cmd=Retrieve&db=PubMed&dopt=Citation&list_uids=14693669)
- Whitsett J A & Weaver T E 2002 *N Engl J Med* **347**(26), 2141–2148.  
<http://content.nejm.org>
- Wolf G K, Grychtol B, Frerichs I, Zurakowski D & Arnold J H 2010 *Pediatr Crit Care Med* **11**(3). In press.